

Spectral Motional Stark Effect Measurements on ASDEX Upgrade

R. Reimer¹, A. Dinklage¹, R. Fischer², B. Geiger², J. Geiger¹, J. Hobirk², A. Kus¹,
T. Löbhard², P.J. Mc Carthy³, A. Mlynek², M. Garcia-Munoz², M. Reich², R. Wolf¹,
the ASDEX Upgrade² and Wendelstein 7-X Team¹

Max-Planck-Institut für Plasmaphysik, ¹Greifswald, ²Garching, Germany

³ *Dept. of Physics, University College Cork, Association EURATOM-DCU, Cork, Ireland*

Introduction

Local measurements of the magnetic field are essential for the reconstruction of plasma equilibria. Typically, motional Stark effect (MSE) polarimetry is employed to derive pitch angles from the central σ emission line [1]. This paper uses the full spectrum due to the Motional Stark Effect (sMSE) to derive information about both the magnetic field strength and its direction. The observation of the MSE spectrum is reported, e.g., in Ref. [2].

This work aims specifically at the assessment of measuring capabilities to investigate the plasma diamagnetism and the role of fast ions for the plasma equilibrium. A spectral MSE diagnostic has been implemented and discharges were performed to assess the measuring capabilities and the effects of different heating scenarios on the creation of fast ions.

Spectral MSE diagnostic on ASDEX Upgrade

Experimental set-up: The detailed features of the diagnostic set-up are described in Ref. [3]. The sMSE diagnostic observes the Doppler-shifted Balmer- α transition from deuterium neutral beam emission. The observation optics consist of a Czerny-Turner spectrometer and a CCD-camera to detect spectrally resolved data at different plasma radii. To suppress the unshifted high intensity neutral hydrogen and deuterium emission, a blocking wire has been placed in the focal plane of the spectrometer. Furthermore, the optical elements of the MSE polarimeter set-up are assessed with respect to their polarizing characteristics.

Data analysis: The detailed forward model for the spectral MSE measurement is described in Ref. [4]. The magnetic field strength causes a splitting of the $n = 3 \rightarrow 2$ transition due to the induced Lorentz field $\vec{E}_L = \vec{v} \times \vec{B}$. The anisotropic intensity distribution of the differently polarized components of the Stark spectrum (π and σ light corresponding to $\Delta m = 0$ and $\Delta m = \pm 1$ transitions) is reflected in intensity modifications captured in the applied forward model by an intensity ratio $T_p = \sum_i I_{\pi_i} / \sum_i I_{\sigma_i}$. In order to calculate absolute values of the pitch angle, non-statistical distributions of the Stark sublevels [5] need to be considered. This deviation can be incorporated by a correction c_{ns} . Furthermore, polarizing effects of the optical components

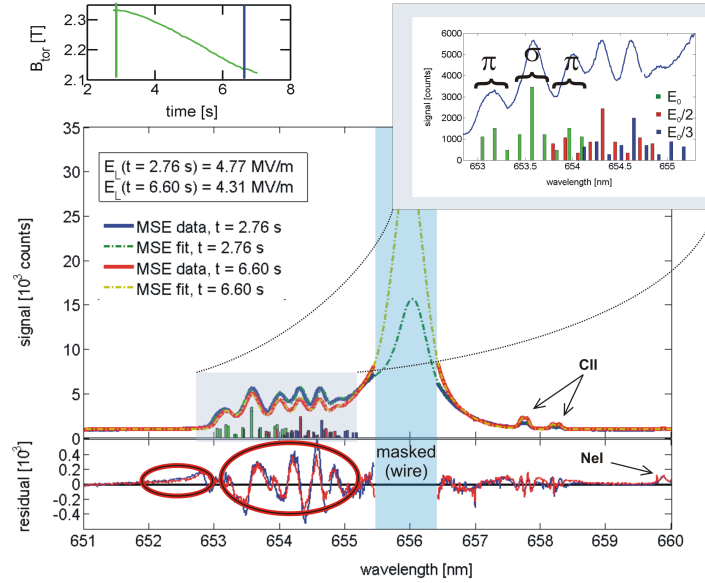


Figure 1: Motional Stark effect spectra from ASDEX Upgrade shot #26322. The inset reflects the multiplet component from full, half and third beam energy.

must be taken into account. This polarizing characteristics are incorporated in c_{optic} . In total, the spectrum yields an apparent intensity ratio $T_p^m = c_{optic} \cdot c_{ns} \cdot T_p$. The main outcome of the fits are the Lorentz field, E_L , and the apparent intensity ratio, T_p^m , as discussed in the next section.

Experimental results from spectral MSE measurements

Fig. 1 displays typical spectra and fitting results for a magnetic field ramp at distinct times at one radial position (channel 5, $R = 1.86$ m). The dominating feature is the charge exchange emission around the unshifted wavelength of the D_α line. Experimentally this spectral region is masked. On the blue-wing side, the Doppler-shifted peaks appear, showing the Stark multiplet corresponding to full, half and third energy beam emission as shown in the inset of Fig. 1. Also impurity lines are observed, e.g. CII. The fit has a remarkably high quality. This high quality allows one to assess small systematic deviations (in figures of the signal amplitude) in much detail. First, a broad background for $\lambda > 652$ nm appears in the residual indicating fast ion charge exchange emission [6]. Second, oscillations in the residual of the fit in the MSE region (653...656 nm) indicate deviations possibly resulting from cross-talks, non-linear dispersion and beam geometry, all of which are presently assessed. For the example in Fig. 1 the magnetic field was varied by $\delta B/B = 9.6\%$. The measured variation from the sMSE gives $\delta E_L/E_L \propto \delta B/B \approx (8.5 \pm 0.3)\%$.

Fig. 2 displays results from spectral MSE measurements for two ASDEX Upgrade discharges ($B = -2.48T$, $I_p = 0.8MA$, $n_e^0 = 6.3 \dots 6.7 \times 10^{19} m^{-3}$). The examples show different heating

scenarios to investigate the potential generation of fast ions and their impact on the equilibrium magnetic field. In discharge #26318, the neutral beam injection was alternating between more

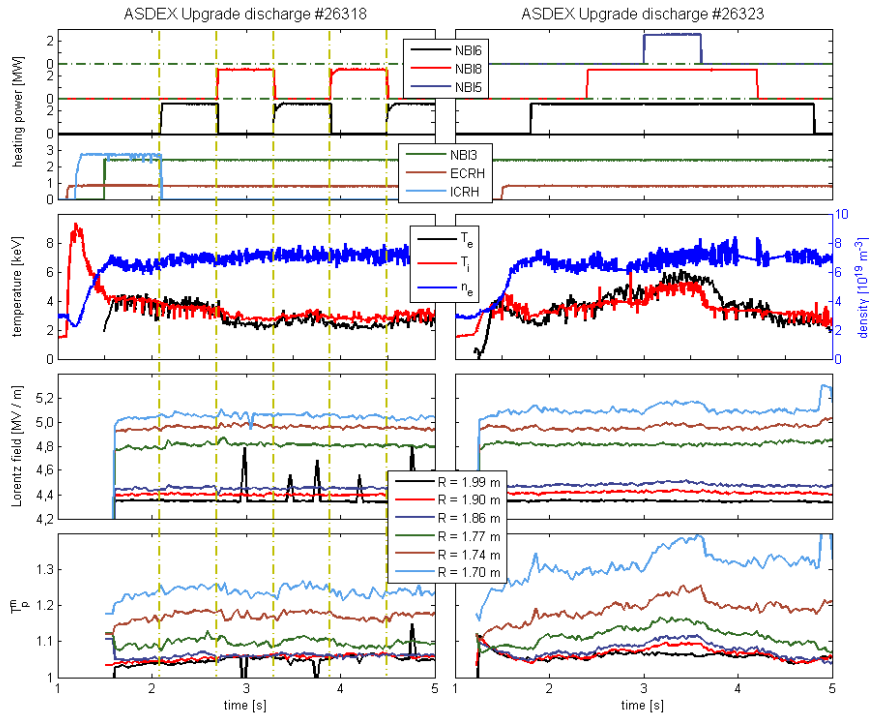


Figure 2: Spectral MSE results: time traces for the measured Lorentz field \vec{E}_L and the apparent polarization ratio T_p^m (third and fourth row) for two ASDEX Upgrade shots (sMSE observed on NBI3). Time traces of the port-through power (P) of applied heating sources is shown in the first row, the second row shows the central electron temperature (T_e) and density (n_e) (IDA [7]) along with ion temperature measurements (T_i) from charge exchange recombination spectroscopy.

radial (NBI8) and more tangential injection (NBI6, cf. Fig. 2 (left)). The power deposition of NBI8 is more on-axis while the deposition of NB6 is more off-axis. The measured Lorentz fields (e.g. (5.05 ± 0.025) MV/m for channel #9) from the Stark splitting differs systematically from +5 % in the center to -5 % towards the edge to the values derived from magnetic field reconstruction of the CLISTE code and the neutral beam geometry [8]. There is no clearly visible effect on the measured Lorentz field resulting from the alternating neutral beam direction/deposition. Differently, the more centrally deposited NBI heating (NBI8) leads to a decrease of the apparent intensity ratio indicating changes in the poloidal field due to the neutral beam injection.

Discharge #26323 in Fig. 2 shows the effect of successively increasing heating power. In addition to the previously discussed heating with NBI6 and NBI8, NBI5 adds additional on-axis deposited heating power. The fourth row of Fig. 2 reflects the stepwise increasing heating power in the apparent intensity ratio T_p^m increasingly towards the plasma center (corresponding

to channels 8 and 9 as the innermost observation channels). Differently to discharge #26318, also the Lorentz field is changing when the maximum heating power is applied. This change is largest for the plasma center. Again this effect is accompanied by largest changes in T_p^m .

In the phase of largest heating power, an increase of the central pressure can be observed from kinetic measurements (second row of Fig. 2(right)). The difference prior and during NBI6 heating ($t = 2.94$ s and $t = 3.55$ s) can be estimated to be $\Delta p_{kin} = (3.6 \pm 0.8) \times 10^4$ Pa. This does not agree even in sign with the diamagnetic pressure change (suggesting a pressure drop) derived from the sMSE measurement $\delta p \approx -\Delta E_L/E_L \times B^2/\mu_0 \approx -(3.7 \pm 0.9) \times 10^4$ Pa and $-(7.6 \pm 0.6) \times 10^4$ Pa for the two central sMSE channels.

Outlook

The spectral MSE diagnostic has been implemented and operated on ASDEX Upgrade. The Stark spectrum could be fitted reasonably well with a forward model. The absolute values of the measured Lorentz field and reconstructed fields from CLISTE differ dependent on the channel from -5 % to 5 % from the outer to the central channels. It still needs to be revealed whether these differences are due to large changes in the current distributions even changing the total field, or effects such as the Shafranov shift. Moreover, fast ion D_α background could contribute to the reconstructed spectrum. The apparent line ratio appears to be very sensitive to small changes in the equilibrium. However, the derivation of non-statistical contributions and polarization properties of the observation optics to resemble the true intensity ratio are required as well and are underway.

References

- [1] F. M. Levinton, G. M. Gammel, R. Kaita, *et al.*, Rev. Sci. Instrum., **61**, 10 (1990)
- [2] W. Mandl, R.C. Wolf, M. G. von Hellermann and H.P. Summers, Plasma Phys. Control. Fusion **35**, 1373 (1993)
- [3] R. Reimer, A. Dinklage, J. Geiger, *et al.*, Contrib. Plasma Phys **50**, 8 (2010)
- [4] A. Dinklage, R. Reimer, R. Wolf, M. Reich, Fusion Sci. Technol. **59**, 406 (2011)
- [5] O. Marchuk, Yu. Ralchenko, R.K. Janev, *et al.*, J. Phys. B **43**, 011002 (2010)
- [6] W. W. Heidbrink, Rev. Sci. Instrum. **81**, 10, (2010)
- [7] R. Fischer, C.J. Fuchs, B. Kurzan, *et al.*, Fusion Sci. Technol. **58**, 675 (2010)
- [8] W. Schneider, P. McCarthy, K. Lackner, *et al.*, Fusion Eng. Des. **48**, 127 (2000)